Arab J Geosci (2017) 10:139
DOI 10.1007/s12517-017-2873-8

ORIGINAL PAPER

Hydrochemical characteristics and evaluation of the granite aquifer in the Alwadeen area, southwest Saudi Arabia

Sattam Almadani[1] · Hussain Alfaifi[1] · Abdullah Al-Amri[1] · Mohamed Fnais[1,2] · Elkhedr Ibrahim[1,4] · Kamal Abdelrahman[1,3] · Mohammed Shehata[5] · Faisal Zaidi[1]

Received: 10 November 2016 / Accepted: 24 January 2017

Abstract This study was carried out in the Alwadeen area of Khamis Mushayt district of southwestern Saudi Arabia to evaluate the hydrochemical characteristics of the shallow hard rock aquifers. These hard rock aquifers mostly comprise granites and contain significant quantities of groundwater that complement the available groundwater from the unconsolidated alluvial sediments in the nearby wadis. The field investigation indicates two main fracture sets which intersect each other and are oriented in the west-northwest and east-west directions. The granitic rocks in the area are intruded by coarse-grained and quartz-rich monzogranite and pegmatite veins. Hydrogeologically, the fracture systems are important since they facilitate the groundwater storage and assume the transmissive function during times of groundwater abstraction. Given the fact that groundwater in the fractured rock aquifers generally occurs at shallow depths, it may be exposed to contamination from surface and/or near-surface sources, and it is therefore important to evaluate its quality. To this end, a hydrochemical analysis was carried out on six groundwater samples collected from the area. The hydrochemistry revealed that the groundwater is fairly fresh, and facies analysis reveals mixed Na-Cl and Ca-Mg-Cl-SO_4 types. Overall, the results reveal that the groundwater is saturated with calcite and dolomite, but unsaturated with gypsum and halite. The degree of salinity increases in the direction of the groundwater flow due to increased rock-water interaction.

Keywords Fractured granite · Geochemical modelling · Flow path · NETPATH · WATEQ4F · Shallow aquifer · Alwadeen area

✉ Kamal Abdelrahman
khassanein@ksu.edu.sa

[1] Geology and Geophysics Department, College of Science, King Saud University, Riyadh, Kingdom of Saudi Arabia

[2] Princess Nourah bint Abdulrahman University, Riyadh, Kingdom of Saudi Arabia

[3] Seismology Department, National Research Institute of Astronomy and Geophysics, Cairo, Egypt

[4] Geology Department, Faculty of Science, Mansoura University, Mansoura, Egypt

[5] Geology Department, Faculty of Science, Zagazig University, Zagazig, Egypt

Introduction

Groundwater supply from hard rock aquifers are common in many parts of the world especially in large areas called shields which comprise mainly igneous and metamorphosed igneous rocks (Marechal et al. 2004). The lack of sufficient surface water resources in arid and semi-arid regions has resulted in the exploitation of shallow groundwater resources; however, the presence of semi-arid or arid climates in hard rock regions increases the complexity related to water availability. In fractured basement rocks, the matrix is impermeable and has no porosity; therefore, groundwater flows only through conduits with the probability of meeting water-bearing fissures decreasing with depth (Cook, 2003; Faillace, 2003). In most cases, regional aquifers do not exist in the hard rock and the groundwater occurs at irregular intervals related to the fracturing and weathering of the rock (Faillace, 2003). The fractures act as conduits for groundwater flow, and their ability to conduct water is affected by the degree to which they are interconnected (Faillace, 2003). Fracture connectivity, meanwhile, increases as fracture length and density increases (Cook, 2003). These weathered and fractured rocks are considered an important source of groundwater and can form reliable

Published online: 20 March 2017

aquifers in many arid areas (e.g. Al-Ahmadi and El-Fiky, 2009; Singhal and Gupta, 1999). Hard rock aquifers across the world have been studied extensively in relation to their hydrodynamic properties (Marechal et al. 2004; Dewandel et al. 2011), water budget (Marechal et al. 2006), hydrogeological conceptual model (Dewandel et al. 2006), understanding the behaviour of groundwater flow (Negrel et al. 2011), processes resulting in the development of secondary porosity (Lachassagne et al. 2011), optimization of the piezometric network (Zaidi et al. 2007) and large-scale mapping of hard rock aquifer properties (Courtois et al. 2010).

The arid environment of Saudi Arabia is characterized by the absence of surface water bodies due to minimal precipitation and high rates of evapotranspiration. Geologically Saudi Arabia can be divided into two distinct geological units: the Precambrian Arabian shield (consisting of igneous and metamorphic rocks) and the Arabian Platform comprising a thick sequence of Palaeozoic to Recent sedimentary succession overlying the basement rocks. The water resources in the Arabian platform are more pronounced thanks to the availability of groundwater reserves stored in the deep-seated sedimentary aquifers. Nevertheless, groundwater resources sufficient to sustain small communities and small-scale agricultural activities are also found in the Arabian shield thanks to the development of secondary porosities in the form of weathering and fracturing of the basement rocks. Since the domestic, agricultural and industrial demand for water depends on the available groundwater, it is very important to understand the groundwater chemistry and the factors which govern this. Rock-water interaction affects the groundwater hydrochemistry, and the variation in major ions helps to identify the geochemical processes that affect the ground water quality (Li et al. 2013, 2016). The occurrence, hydrochemistry and composition of groundwater in fractured hard rocks have been assessed in various areas around the world (Senthilkumar and Elango, 2013; Raju et al., 2011; Kirchner, 2009; Holland and Witthüser, 2009; Sami, 2009; Al-Ahmadi and El-Fiky, 2009, Seung-Gu, 2008; Faillace 2003). In the Arabian shield, however, the groundwater chemistry and its controlling factors are still poorly understood.

The available water supplies in fractured hard rock aquifers are limited due to the low porosity of the aquifer matrix and, at the same time, the high permeability due to the presence of tectonic fractures. Furthermore, their origin in weathering makes these aquifers vulnerable to pollution due to household and industrial sewage disposal on the surface. Keeping these facts in mind, the main objectives of the present study were to investigate the groundwater quality and to assess the main hydrological processes regulating the overall groundwater chemistry in a shallow groundwater aquifer in the Alwadeen area of Khamis Mushayt City in southwestern Saudi Arabia.

Geologic setting of the study area

The investigated area is located in southwestern Saudi Arabia between latitudes 18° 06′ 30″N and 18° 07′ 30″ N and longitudes 42° 47′ 40″ E and 42° 48′ 30″E. The studied area is marked as a square in Fig. 1. It belongs to the granitic terranes of the pre-Pan-African structures that developed in association with the formation, amalgamation and accretion of oceanic volcano-sedimentary terranes (Nehlig et al., 2002). Many authors have shown that the Arabian shield relates to Pan-African (690–590 Ma) and pre-Pan-African (>690 Ma) structures that partly obscure the earlier structures (Johnson et al., 2013; Johnson and Kattan, 2012). The granitic rock unit that dominates the study area consists of plagioclase, microcline, quartz and biotite and, locally, grades into tonalite and monzogranite, biotite—hornblende granodiorite to monzogranite and biotite monzogranite. Biotite and monzogranite rocks form large plutons NW of the area. The granitic unit includes subordinate granodiorite that is pink to medium grey, medium to course grained and massive to weakly cleaved. It is composed of quartz, oligoclase, microcline and biotite.

The field investigation indicated that the study area is covered with fractured and jointed diorite, granodiorite and granitic rocks. These fractures intersect the country rocks in the west-northwest and east-west directions (Fig. 2). The west-northwest-directed fractures are of tertiary age and are related to the Red Sea rifting, or were reactivated during the Phanerozoic (Motti et al., 1982 and Blank 1977). The bi-directional rose diagram graphical method has been used to display the fracture orientation as determined from the exposed granitic rock units in the study area (Fig. 3). Sixty-three fractures were used to prepare the rose diagram. The dominant fracture orientations can be subdivided into two major sets: those directed in the N100E and N150E directions.

In some places, the granite is intruded by pegmatite and coarse-grained, quartz-rich, quartzite veins. These veins and the resulting coarse-grained weathering product could develop open joint systems between the granitic blocks (Fig. 4a). Many vertical or steeply inclined dykes intrude the pre-existing granite country rocks with widths ranging from centimetres to half a metre (Fig. 4b). Mafic dikes are composed of basalt, diabase and subordinate diorite that are metamorphosed to amphibolite and greenschist facies. The felsic dikes are light-coloured, fine to coarse-grained monzogranite, porphyritic rhyolite to dacite and pegmatite (Fig. 4b). Locally, some of these dikes are strongly foliated and extend parallel to their contacts (Fig. 4c).

Fig. 1 Geological map of the Alwadeen area with a *square* showing the studied area and the locations of the shallow groundwater wells ▶

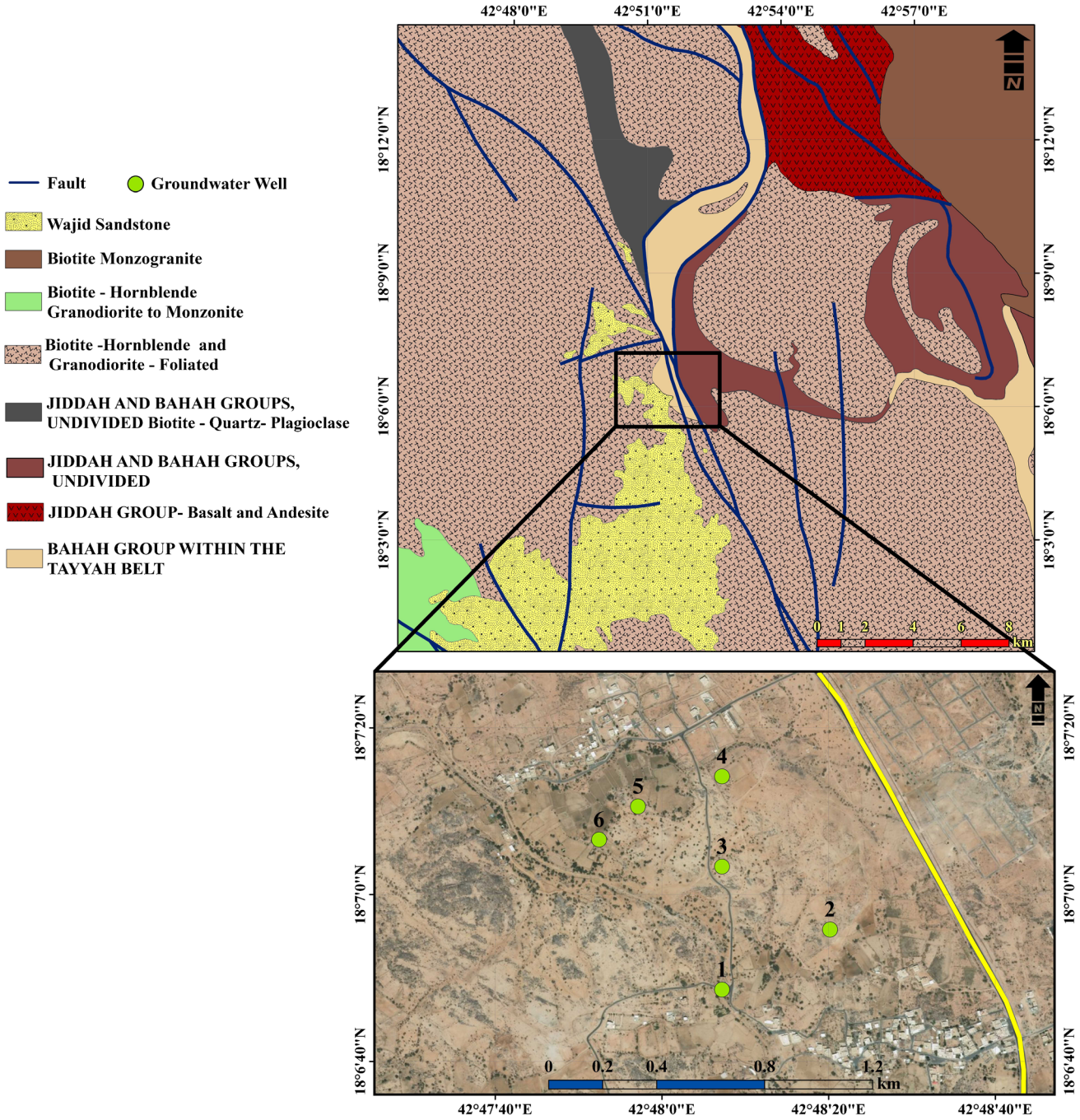
Fault
Groundwater Well
Wajid Sandstone
Biotite Monzogranite
Biotite - Hornblende Granodiorite to Monzonite
Biotite -Hornblende and Granodiorite - Foliated
JIDDAH AND BAHAH GROUPS, UNDIVIDED Biotite - Quartz- Plagioclase
JIDDAH AND BAHAH GROUPS, UNDIVIDED
JIDDAH GROUP- Basalt and Andesite
BAHAH GROUP WITHIN THE TAYYAH BELT
42°48'0"E
42°51'0"E
42°54'0"E
42°57'0"E
18°12'0"N
18°9'0"N
18°6'0"N
18°3'0"N
N
0 1 2 4 6 8 km
18°7'20"N
18°7'0"N
18°6'40"N
42°47'40"E
42°48'0"E
42°48'20"E
42°48'40"E
1
2
3
4
5
6
0 0.2 0.4 0.8 1.2 km

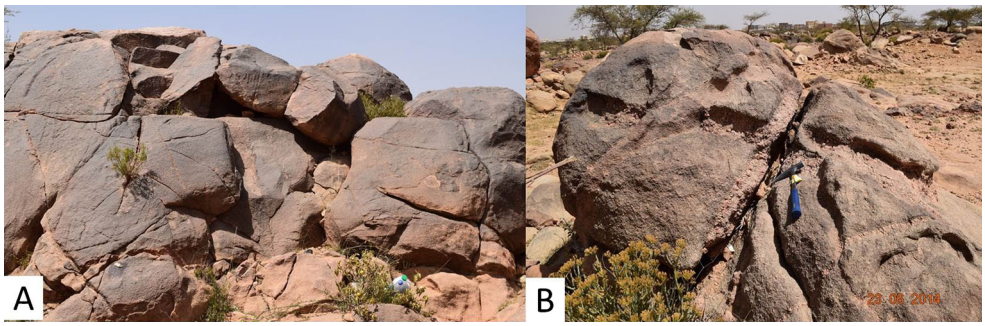

Fig. 2 **a**, **b** Field photos showing fractures in the granitic rocks in the Alwadeen area, southwest Saudi Arabia

The geometry of the structures in the studied area is quite diverse due to the lithological variations. These outcropped basement granitic rocks and associated structures are covered in many places by a thin layer of alluvium deposits that range from silty sand to gravely soil (Fig. 5). This alluvial layer reaches its maximum thickness in the NW of the studied area.

Methodology

In this study, a total of six water samples were collected and analysed from the available shallow-dug wells. The number of samples was limited by the limited number of available wells.

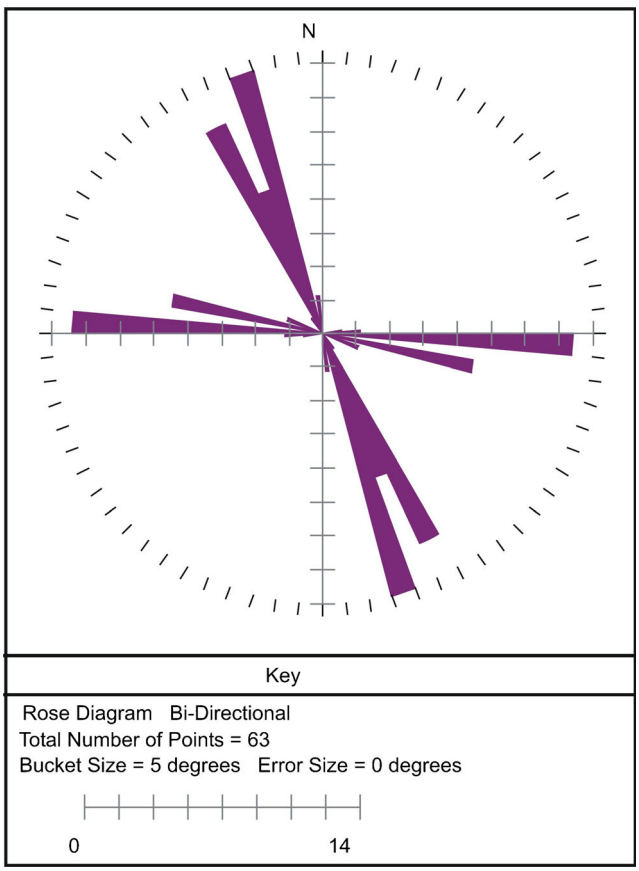

Fig. 3 Rose diagram of the orientations of 63 fractures measured in the field of Alwadeen granite, southwest Saudi Arabia

The present study was carried out in an area that is considered to be an urban extension area for two surrounding villages (with a total area of 1.5 × 1.2 km^2), and the local people depend on the groundwater as their main source of drinking and irrigation water. The depth to the water table varies between 2 and 8 m (Fig. 6). The watershed boundary and flow pattern in the basin for the study area is illustrated in Fig. 7.

Samples were collected in rinsed plastic bottles to prevent any contamination. For in situ measurement of pH, temperature and electrical conductivity (EC), a Thermo Scientific Orion 5-Star instrument was used. The standard methods described by the American Public Health Association were followed for sample preservation and analysis. The nitrate and fluoride concentrations were measured in the central laboratory facility at the College of Science in King Saud University, Riyadh. The hydrochemical facies of the analysed water samples were assessed using a Piper plot.

Groundwater chemical reaction systems, such as precipitation and dissolution of solids, ion exchange and sorption by clay minerals, can be calculated and modelled using geochemical models. Inverse and forward modelling can be used to model the groundwater aquifer geochemical interactions (Plummer 1984). According to Deutsch (1997), the added reactants will dissolve if they are undersaturated in this solution. The forward model can be described as follows:

$$IS + R = PS + P$$

where

IS denotes the initial solution
R denotes the reactants
PS denotes the predicted solution
P denotes the products

The amount of reactants (in mmol/kg of H_2O) dissolved in the water samples and the amount of products deposited from the solution were calculated. The produced solution was controlled either by the mass of reactants added or the solubility of the mineral product.

NETPATH software (El-Kadi et al., 2010) was used to evaluate the geochemical processes and to conduct a

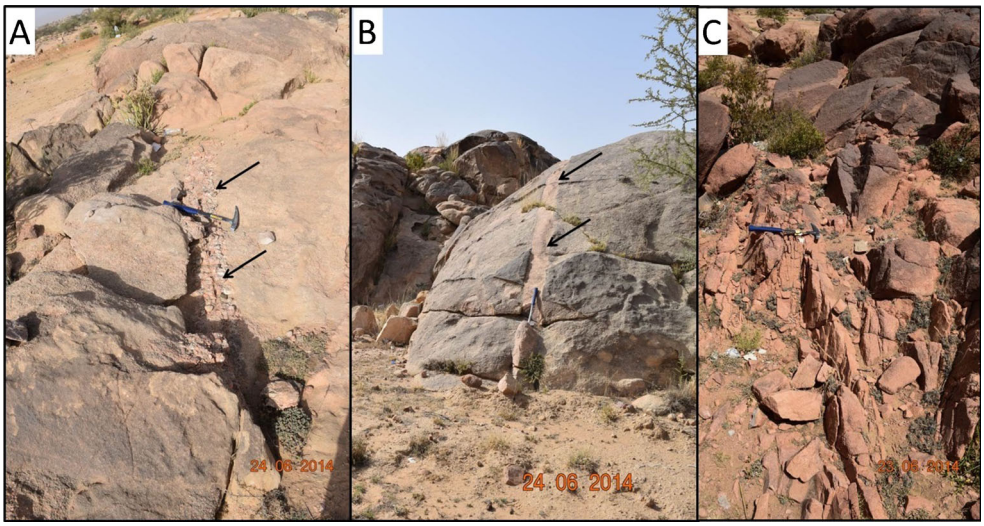

Fig. 4 **a**–**c** Field photos showing dike veins intruded in the granitic rocks in the Alwadeen area

variety of aqueous geochemical calculations, such as testing of water corrosivity, saturation indices (SI) of the major mineral phases, and to apply water mixing models. Using NETPATH, the net geochemical mass-balance reactions between initial and final waters along a hydrologic flow path can be interpreted (Plummer et al., 1991) thereby indicating the potential of the reaction system. A modified version of the aqueous speciation program, WATEQ4F (Ball and Nordstrom, 1992), was used as a part of the NETPATH model input data and also for the calculation of saturation indices.

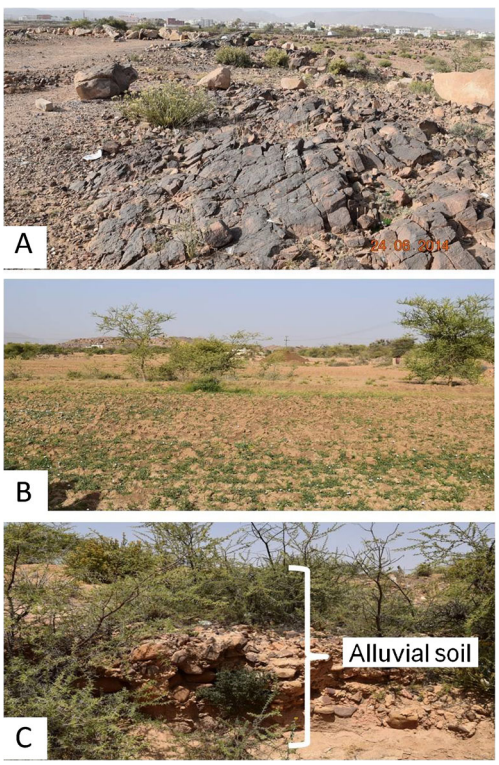

Fig. 5 **a**–**c** Alluvium soil section covering the fractured granitic rock unit

Results and discussion

Total dissolved solids (TDS) measure the "freshness" of water. Drinking water classification was discussed according to TDS and major ion guidelines (WHO, 2006). The results for total dissolved solids indicate that the studied groundwater samples range from fresh to brackish water. Groundwater with high TDS indicates that water-rock interaction occurs between water and water-bearing formations.

The groundwater samples (nos. 3–6) had low electrical conductivity (EC < 1000 μS/cm), indicating weakly mineralized (granite terrain) to highly mineralized water (Table 1). Groundwater samples (nos. 1 and 2) exhibited excessively

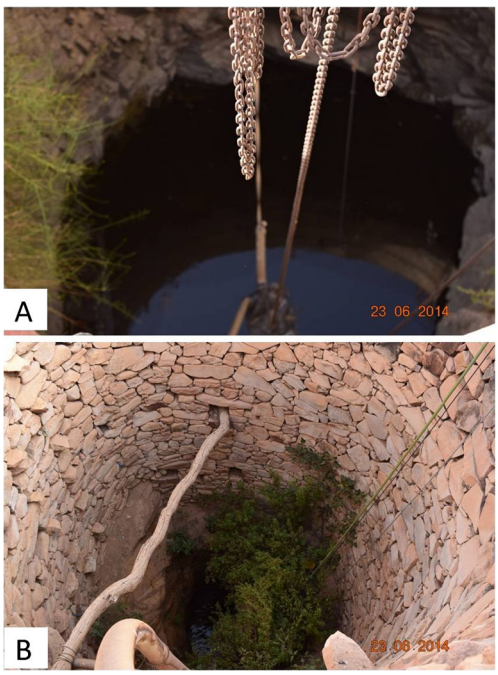

Fig. 6 **a**, **b** Shallow-dug wells with different groundwater levels in the study area

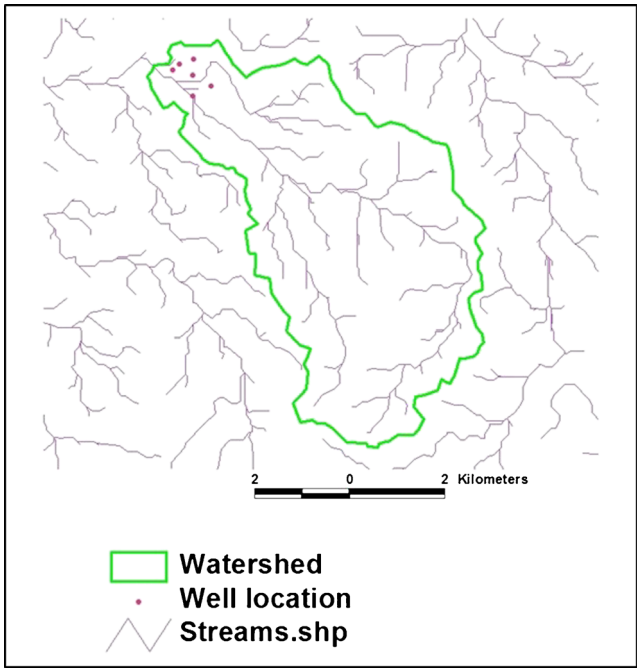

Fig. 7 Watershed boundary and flow pattern in the study area

mineralized water (EC > 1000 μS/cm). This variation in the EC is attributed to geochemical processes, such as evaporation, ion exchange, silicate weathering and water-rock interaction processes. Total hardness was also assessed. For sample nos. 3–6, $CaCO_3$ was 150–300 mg/l, showing that the water was hard, whereas samples 1 and 2 had values >300 mg/l, showing very hard water. The resulting data indicates that the total hardness increases as the level of mineralization in the water increases. The fact that water hardness increases as water salinity increases could be due to the leaching and dissolution of salts indicating an increase in hardness, with the concentration of NaCl having a particular effect on the Ca^{2+} solubility and Mg^{2+} in the water (Hem, 1989, Freeze and Cherry, 1979).

Hydrochemical facies

The chemical properties of the groundwater samples show primary salinity and noncarbonate alkalis indicating chemical properties dominated by alkalis and strong acids and by (SO_4 + Cl > Na + K). A Piper plot was prepared to determine the groundwater facies. The groundwater is essentially meteoric water, but with increasing Ca + Mg, it changes to mixed meteoric water (Fig. 8). The resulting triangle shows that one sample falls within the Ca-dominant type, another one falls in the Na + K-dominant type and the remaining four samples have no dominant type. On the other hand, the anionic triangle shows three samples falling within the bicarbonate-dominant type and the other three as having no dominant type. Based on the cation and anion combinations, three main groundwater facies can be identified in the diamond of the Piper plot. Facies 1 of the $CaHCO_3$ type, indicating freshly recharged or meteoric water, is represented by three samples. Since the area receives a higher precipitation compared to the other arid regions of the Arabian Peninsula, and is characterized by a shallow weathered fractured aquifer system, a fresh groundwater recharge signature can be expected. Two samples fall into the facies 2 type, characterized by the mixed Ca-Mg-Cl-SO_4 type of groundwater. One sample falls into the Na-Cl type of groundwater facies (facies 3). The direction of the arrow on the Piper plot represents the general direction of groundwater flow. Increased rock-water interaction takes place along the flow direction, as a result of which the groundwater loses its initial meteoric signature.

Table 1 Hydrochemical analyses of groundwater samples in the study area

Well no.	pH	E.C. μS/cm	TDS mg/l	TH mg/l	Alk. mg/l	Cations				Anions					Water type
						K^+ mg/l	Na^+ mg/l	Ca^{2+} mg/l	Mg^{2+} mg/l	Cl^- mg/l	SO_4^{2-} mg/l	HCO_3^- mg/l	NO_3^- mg/l	F^- mg/l	
1	7.68	2380	1654	684	290	4.9	287	198	46	294	429	290	189	1.6	Na-Ca-SO_4-Cl
2	7.48	1678	1072	431	170	6.4	223	118	33	266	293	170	100	1.7	Na-Ca-Cl-SO_4
3	7.69	925	560	279	206	2.2	84	83	17	72	83	206	92	1.6	Ca-Na-HCO_3-Cl
4	7.49	648	362	266	250	2.3	52	78	17	37	52	250	30	1.0	Ca-Na-HCO_3
5	7.53	805	480	237	282	3.1	70	70	15	45	79	282	14	1.5	Ca-Na-HCO_3-SO_4
6	7.67	920	584	313	258	3.0	106	99	16	47	111	258	46	2.2	Ca-Na-HCO_3-SO_4

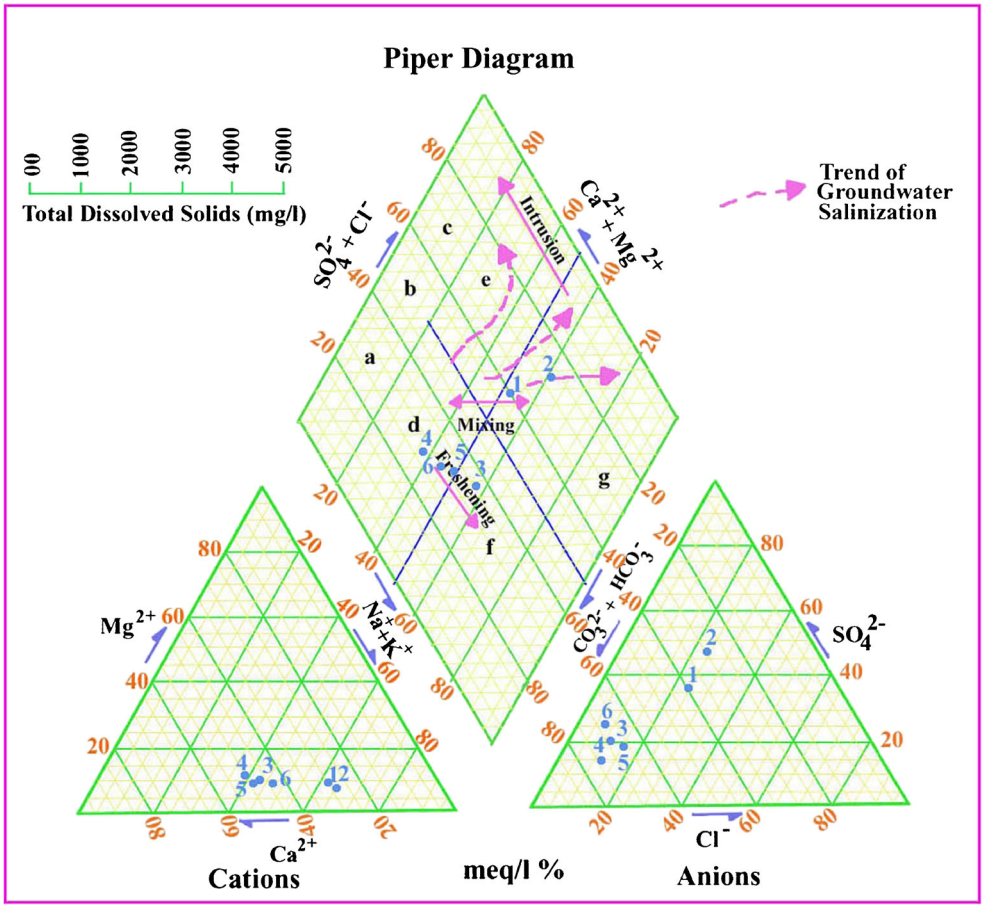

Fig. 8 Piper diagram showing the different groundwater compositions in the study area

Hydrochemical modelling

The collected samples (Table 1) were analysed using NETPATH modelling to determine the geochemical evolution through the flow path of the groundwater. The water moves through different geological units and aquifers during its journey of infiltration, until it reaches the recharge area where it reacts with the different mineral assemblages encountered in the aquifer strata. This journey, and the associated reactions, affect and control the chemistry of the groundwater. The groundwater containing CO_2 infiltrates vertically into the unsaturated zone and is altered chemically before reaching the saturated zone. This process occurs in the recharge area and seasonal runoff and is caused by the uptake of soil CO_2 by pore water to form $H_2CO_3^0{}_{aq}$, HCO_3^- and CO_3^{2-} (Table 2). These reactions control the alkalinity and pH in the groundwater system (reaction no. 1, Table 2) under the partial pressure of CO_2 (P_{CO_2}) in soil pores. If the void space in the pores has a sufficient mass of CO_2, the P_{CO_2} does not change significantly as the reactions proceed.

In order to evaluate the geochemical processes of the groundwater as it flows from the recharge area to the discharge area, in the present study, representative samples were collected from the recharge area as the initial water (well no. 4) and other samples were selected from the final waters in the same aquifer and in the direction of the groundwater flow path (well no. 1). The flow path which represents the Na-SO_4 water types was used to evaluate the shallow groundwater aquifer in the study area. Changes in chemical composition and mineral saturation indices were observed in the collected samples along the flow paths (Table 3).

Table 2 List of chemical reactions used in the present study

No.	Reactions
1	$CO_2\ (g) + H_2O \leftrightarrow H_2CO_3^0{}_{aq}$
2	$H_2CO_3^0{}_{aq} \leftrightarrow H^+ + HCO_3^-$
3	$HCO_3^- \leftrightarrow H^+ + CO_3^{2-}$
4	$CaCO_3 + H_2CO_3 \leftrightarrow Ca^{2+} + 2HCO_3^-$
5	$CaMg\ (CO_3)_2 + 2H_2CO_3^0{}_{aq} \leftrightarrow Ca^{2+} + Mg^{2+} + 4HCO_3^-$
6	$CaMg\ (CO_3)_2 + 2H_2CO_3^0{}_{aq} \leftrightarrow CaCO_3 + Mg^{2+} + 2HCO_3^-$
7	$CaSO_4{\cdot}2H_2O \leftrightarrow Ca^{2+} + SO_4^{2-} + 2H_2O$
8	$HCO_3^- \leftrightarrow H^+ + CO_3^{2-}$
9	$H^+ + HCO_3^- \leftrightarrow H_2CO_3$
10	$Ca^{2+} + HCO_3^- \leftrightarrow CaHCO_3$
11	$CaMg\ (CO_3)_2 + CaSO_4 \leftrightarrow 2CaCO_3 + MgSO_4^0{}_{aq}$

Table 3 WATEQ4F analytical data and calculated data for the initial and final water wells from the study area; Na-SO_4 flow path in the shallow aquifer

Variables	Initial water (well no. 4) Concentrations (mg/l)		Final water (well no. 1) Concentrations (mg/l)	
	Calculated	Analysed	Calculated	Analysed
Ca^{2+}	76.92	78	199.25	198
$CaCO_3^0{}_{aq}$	1.31		3.03	
CaF	0.09		0.13	
$CaHCO_3$	13.70		6.16	
$CaSO_4^0{}_{aq}$	118.25		125.32	
Cl^-	38.12	37	295.25	294
NO_3^-	29.04	30	187.85	189
F^-	1.57	1.0	2.05	1.6
$HCO_3^0{}_{aq}$	20.93		2.25	
$H_4SiO_4^0{}_{aq}$	51.17		39.02	
HCO_3^-	251.95	250	251.74	250
K^+	2.78	2.3	5.82	4.9
KSO_4	0.73		1.50	
Mg^{2+}	16.82	17	45.28	46
$MgCO_3^0{}_{aq}$	0.37		0.91	
MgF	0.28		0.46	
$MgHCO_3$	6.15		2.92	
MgOH	$2.6 * 10^{-3}$		$1.2 * 10^{-2}$	
$MgSO_4^0{}_{aq}$	155.99		134.99	
Na^+	51.42	52	286.25	287
$NaCO_3$	0.04		0.22	
$NaF^0{}_{aq}$	0.01		0.01	
$NaHCO_3^0{}_{aq}$	0.99		1.17	
$NaSO_4$	16.04		48.09	
SO_4^{2-}	55.86	52	431.83	429
TIC (mol/l)	$3.75 * 10^{-3}$		$2.04 * 10^{-3}$	
pH	7.85	7.49	8.05	7.68
Ionic Str.	$4.5 * 10^{-2}$		$5.4 * 10^{-2}$	
P_{CO_2}	$1.0 * 10^{-2}$		$1.1 * 10^{-3}$	
Alkalinity	248.13	250	287.33	290
Calcite SI	0.253		0.752	
Dolomite SI	0.274		0.844	
Gypsum SI	−0.581		−0.223	
Halite SI	−4.392		−5.273	
Palygorskite SI	−1.014		0.374	

Na-SO_4 water type evolution in the studied aquifer

The Na-SO_4 flow path at the initial well indicates a high P_{CO_2} ($1.1 * 10^{-2}$ atm), pH of 7.85 and an alkalinity of 250 mg/l (as $CaCO_3$). On the other side, it reaches the final well with a P_{CO_2} of $1.1 * 10^{-3}$ atm, pH of 8.05 and alkalinity of 290 mg/l (as $CaCO_3$) (Table 3). According to the calcite and dolomite dissolution, HCO_3^-, and consequently the alkalinity, of the aquifer water increases as it flows. So, the HCO_3^- ions that resulted from the dissolution of carbonate minerals are consumed so as to maintain the concentration of the $H_2CO_3^0{}_{aq}$ in the aquifer water (the reverse of reaction no. 2, Table 2).

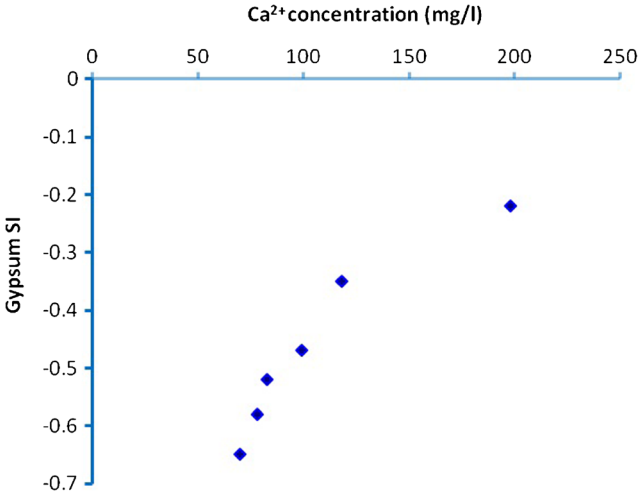

Fig. 9 The relationship between total concentration of Ca^{2+} and gypsum SI for the Na-SO_4 water type of the shallow aquifer in the study area

The gypsum saturation index in the Na-SO_4 flow paths indicates the absence of gypsum phases as continuous beds in the studied shallow aquifer. The relationship between gypsum SI and Ca^{2+} (Fig. 9) indicates the occurrence of a dedolomitization process, where $CaCO_3^0{}_{aq}$ decreases and Ca^{2+} increases as the gypsum saturation indices (SI) increase.

Table 4 summarizes the constraints and plausible phases that can be included in mass-balance modelling of the shallow aquifer. Negative and positive mass transfers indicate precipitation and dissolution of solids, respectively. The set of reactants and products of the aquifer were chosen, and the reaction models are consistent with all the chemical observations for this aquifer system.

The data from the initial and final water wells was entered into NETPATH in order to calculate the mass transfer of plausible phases, and six models were tested for each final water sample in the shallow aquifer. More constraints were

Table 4 Chemical formula and mass-balance reactions of plausible phases in the shallow aquifer, where the reactions are written with anhydrous salts because the NETPATH model assumes a constant mass of 1 kg of water

Phases	Reactions
Dolomite	$CaMg(CO_3)_2 \rightarrow Ca^{2+} + Mg^{2+} + CO_3^{2-}$
Gypsum	$CaSO_4 \rightarrow Ca^{2+} + SO_4^{2-}$
Halite	$NaCl \rightarrow Na^+ + Cl^-$
Calcite	$CaCO_3 \rightarrow Ca^{2+} + CO_3^{2-}$
Palygorskite	$Mg_2(H_4SiO_4)_3 \rightarrow 2\ Mg^{2+} + 3H_4SiO_4$

Table 5 Saturation index of the various mineral species in the analysed samples

Well no.	Calcite	Dolomite	Gypsum	Halite	Palygorskite
1	0.752	0.844	−0.223	−5.273	0.374
2	0.650	0.793	−0.354	−6.014	0.323
3	0.371	0.142	−0.524	−5.711	−1.982
4	0.253	0.274	−0.581	−4.392	−1.014
5	0.281	0.542	−0.653	−4.980	−1.072
6	0.312	0.480	0.471	−5.123	−1.120

introduced into NETPATH for the precipitation and dissolution of each phase.

Saturation indices

The saturation index (SI) describes the saturation status of the minerals in groundwater (Li et al. 2010). An SI of 0 indicates the equilibrium state of the mineral in groundwater, whereas a saturation index of less than 0 indicates a state of undersaturation and an index of more than 0 indicates oversaturation of the mineral in groundwater. Undersaturated states will result in mineral dissolution in groundwater, while oversaturation will result in precipitation of the mineral in groundwater (Qian and Ma 2005; Deutsch 1997). The saturation index SI is defined as follows:

$$\mathrm{SI} = \log(I_{\mathrm{AP}}/K)$$

where

I_{AP} is the ion activity product
K is the equilibrium constant of mineral dissolution at a given temperature.

The saturation indices of the various minerals were calculated using the NETPATH flow model and are given in Table 5. This shows that the water samples are saturated with dolomite and calcite whereas they are undersaturated with gypsum and halite. The absence of gypsum-bearing rocks explains the undersaturation of water with respect to gypsum; however, halite dissolution also takes place along the flow direction. This undersaturation of halite explains the increasing rock-water interaction along the groundwater flow direction resulting in higher TDS values and the evolution of groundwater in which the carbonates in solution are gradually replaced by chlorides (facies 2 and 3 on the Piper plot).

The results indicate that the final water lies between saturation and undersaturation ($0 > \mathrm{SI} > -0.5$) relative to dolomite, which appears in the NETPATH models to be dissolved rather than precipitated. This can be related to the de-dolomitization that retains the calcite equilibrium in the final waters by the dissolution of dolomite and gypsum (reaction no. 11, Table 2). This reaction precipitates 2 mol of calcite for every mole of dissolved dolomite and gypsum. The actual ratios are generally greater than those in the NETPATH models, indicating that the de-dolomitization process starts after calcite reaches equilibrium in the solution by direct precipitation so as to maintain this equilibrium status.

Table 6 Total precipitated calcite in the shallow aquifer as a function of direct precipitation from water reaching equilibrium and as a function of the de-dolomitization process to maintain this equilibrium (in mmol/kg of H_2O)

Well no.	Directly precipitated calcite	Precipitated calcite from de-dolomitization	Total precipitated calcite
1	1.86	2.56	4.42
2	1.81	2.04	3.85
3	1.76	1.84	3.60
4	1.72	0.77	2.49
5	1.70	1.13	2.83
6	1.75	1.63	3.38

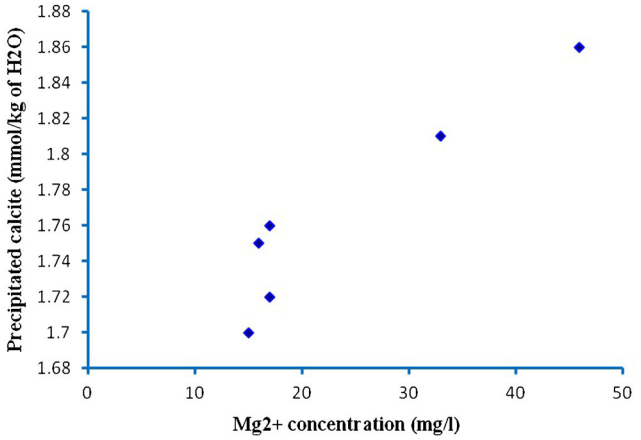

Fig. 10 The relationship between total concentration of Mg^{2+} and precipitated calcite as a function of the de-dolomitization of the shallow aquifer in the study area

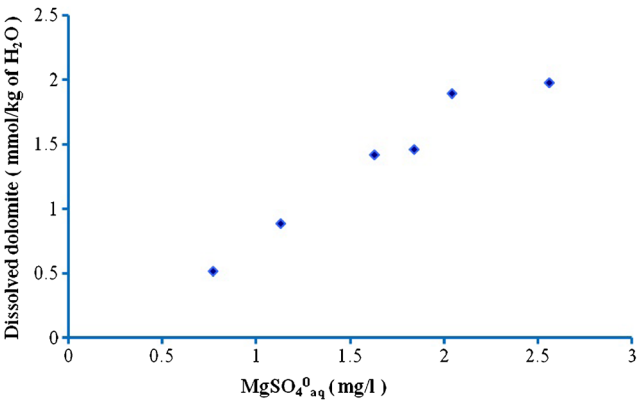

Fig. 11 The relationship between dissolved dolomite and $MgSO_4{}^0{}_{aq}$ as a function of the de-dolomitization process of the shallow aquifer in the study area

Depending on the NETPATH models, the total amount of precipitated calcite can be estimated as follows:

total precipitated calcite = de-dolomitization products + calcite precipitated,

where *de-dolomitization products = 2 * dissolved dolomite*.

The *dissolved dolomite* and *total precipitated calcite* are calculated in the NETPATH models in (mmol/kg of H_2O) for the studied wells (Table 6). The results indicate that the groundwater precipitates corresponding amounts of calcite to reach equilibrium through de-dolomitization, thus maintaining the equilibrium condition by precipitating more calcite according to the following formula: $A/2\ CaMg(CO_3)_2 + A/2\ CaSO_4{}^0_{aq} \rightarrow A\ CaCO_3 + A/2\ MgSO_4{}^0_{aq}$

where A is the precipitated calcite from the de-dolomitization process (Table 6). The total mass transfers of direct calcite precipitation, meanwhile, can be derived by multiplying the following reaction by B:

$$Ca^{2+} + HCO_3^- \rightarrow CaCO_3 + H^+$$

where B is directly precipitated calcite (Table 6). These relationships are represented by plotting total Mg^{2+} against calcite precipitated as a function of the de-dolomitization process, and this shows a good positive correlation (Fig. 10). This means that the de-dolomitization process is the main process in producing calcite in the aquifer along the flow path. This relationship demonstrates that 2 mol of calcite is precipitated for each mole of dissolved dolomite, which is a similar reaction to no. 11 in Table 2. Figure 11 also supports the occurrence of a de-dolomitization process in this type of water through the positive correlation between $MgSO_4{}^0_{aq}$ and the dissolved dolomite phase.

Conclusions

The main aquifer in the Alwadeen area of southwest Saudi Arabia consists largely of shallow weathered/fractured coarse-grained granites. Groundwater facies analyses of six groundwater samples from shallow-dug wells reveal the presence of three types of facies: the Ca-HCO_3 type, the mixed Ca-Mg-Cl-SO_4 type and the Na-Cl type. The presence of the Ca-HCO_3 type of groundwater facies is indicative of fresh groundwater recharge. Comparatively high precipitation rates and the shallow water table explain the presence of this recharge water. Rock-water interaction also takes place along the direction of the groundwater flow; however, as a result of which, the groundwater loses its meteoric signature and shows high TDS values.

The accepted models reflect that Na^+ ions exceed Cl^- in the studied samples from the granite aquifer, indicating ion exchange and dissolution as the main processes along the flow path of the Na-SO_4 water type. The flow path of the Na-SO_4 is characterized by undersaturation of halite and gypsum. The gypsum saturation index reflects the fact that gypsum phases are absent as a continuous bed in the study aquifer. Increasing salinity along the flow direction is explained by the fact that the samples are undersaturated with respect to halite and are capable of dissolving more Na and Cl along the direction of groundwater flow.

Groundwater samples belonging to facies 1 indicate saturation with respect to dolomite and calcite, whereas those belonging to facies 2 and 3 showed a saturation index between saturation and undersaturation ($0 > SI > -0.5$) with respect to dolomite. This is explained by the de-dolomitization process which helps in maintaining the calcite equilibrium in the final waters (facies 2 and 3) by the dissolution of dolomite and gypsum, so the weathered aquifer makes it vulnerable to sewage.

Acknowledgments The authors would like to extend their sincere appreciation to the Deanship of Scientific Research at King Saud University for funding this research group, No. RG-1435-035.

References

Al-Ahmadi ME, El-Fiky AA (2009) Hydrogeochemical evaluation of shallow alluvial aquifer of Wadi Marwani, western Saudi Arabia. Journal of King Saud University 21:179–190

Ball, J.W. and Nordstrom, D.K. 1992. WATEQ4F: a program for the calculating speciation of major, trace and redox elements in natural waters. International Ground Water Modeling Center (IGWMC). U.S.A.

Blank, H. R., 1977. Aeromagnetic and geologic study of Tertiary dikes and related structures on the Arabian margin of the Red Sea. In Hilpert, L.S., ed., Red Sea research 1970–1975, Saudi Arabian Directorate General of Min. Res. 22, G1-G18.

Cook, P. G. 2003. A guide to regional groundwater flow in fractured rock aquifers. National Library of Australia Cataloguing-in-Publication entry. p. 115.

Courtois N, Lachassagne P, Wyns R, Blanchin R, Bougaïré FD, Somé S, Tapsoba A (2010) Large-scale mapping of hard-rock aquifer properties applied to Burkina Faso. Ground Water 48(2):269–283

Deutsch WJ (1997) Groundwater chemistry: fundamentals and applications of contamination. Lewis CRC Press LLC. U. S. A, p 221

Dewandel B, Lachassagne P, Wyns R, Maréchal JC, Krishnamurthy NS (2006) A generalized 3-D geological and hydrogeological conceptual model of granite aquifers controlled by single or multiphase weathering. J Hydrol 330(1):260–284

Dewandel B, Lachassagne P, Zaidi FK, Chandra S (2011) A conceptual hydrodynamic model of a geological discontinuity in hard rock aquifers: example of a quartz reef in granitic terrain in South India. J Hydrol 405(3):474–487

El-Kadi AI, Plummer NL, Aggarwal P (2010) NETPATH-WIN: an interactive user version of the mass-balance model, NETPATH. Department of Geology and Geophysics and Water Resources Research Centre, University of Hawaii at Manoa, Honolulu, Hawaii 96822(808):956–6331

Faillace C (2003) Hydrogeology of hard rocks in some eastern and western African countries. Czech Republic, Groundwater in Fractured Rocks Proceedings. Prague, pp 7–10

Freeze, A.R., Cherry, J. A. 1979. Groundwater. Prentice - Hall, Inc. Englewood Cliffs, New Jersey, p. 604

Hem, J.D. 1989. Study and interpretation of the chemical characteristics of natural waters. 3rd Edition. US Geol. Surv., Water-Supply Paper 2254.

Holland, M., Witthüser, K. 2009. Factors that control sustainable yields in the Archean basement rock aquifers of the Limpopo province. The Basement Aquifers of Southern Africa Proceedings. Rian Titus, Hans Beekman, Shafick Adams and Leslie Strachan (editors), 67-p. 79

Johnson, P.R., Kattan, F.H., 2012. The geology of the Saudi Arabian shield; Saudi Geological Survey: Jeddah, Saudi Arabia, 1–479.

Johnson PR, Halverson GP, Kusky TM, Stern RJ, Pease V (2013) Volcano sedimentary basins in the Arabian-Nubian shield: markers of repeated exhumation and denudation in a Neoproterozoic Accretionary Orogen. Geosciences 3:389–445

Kirchner, J. 2009. Basement aquifer groundwater recharge, storage and flow. The Basement Aquifers of Southern Africa Proceedings. Rian Titus, Hans Beekman, Shafick Adams and Leslie Strachan (editors), 58-66p.

Lachassagne P, Wyns R, Dewandel B (2011) The fracture permeability of hard rock aquifers is due neither to tectonics, nor to unloading, but to weathering processes. Terra Nov. 23(3):145–161

Li P, Qian H, Wu J, Ding J (2010) Geochemical modeling of groundwater in southern plain area of Pengyang County, Ningxia, China. Water Science and Engineering 3(3):282–291. doi:10.3882/j.issn.1674-2370.2010.03.004

Li P, Qian H, Wu J, Zhang Y, Zhang H (2013) Major ion chemistry of shallow groundwater in the Dongsheng coalfield, Ordos Basin, China. Mine Water Environ 32(3):195–206. doi:10.1007/ s10230-013-0234-8

Li P, Zhang Y, Yang N, Jing L, Yu P (2016) Major ion chemistry and quality assessment of groundwater in and around a mountainous tourist town of China. Exposure and Health:1–14. doi:10.1007/ s12403-016-0198-6

Motti, E., Teixido, L., Vazques-Lopez, R. and Vial, A., 1982. Maqna Massif area: geology and mineralization. Saudi Arabian Deputy Ministry for Mineral Resources Open File Report BRGM-OF-02-16, p 44.

Negrel P, Pauwels H, Dewandel B, Gandolfi JM, Mascré C, Ahmed S (2011) Understanding groundwater systems and their functioning through the study of stable water isotopes in a hard-rock aquifer (Maheshwaram watershed, India). J Hydrol 397(1):55–70

Nehlig P, Genna A, Asfirane F (2002) A review of the Pan-African evolution of the Arabian shield. GeoArabia 7:103–124

Plummer LN (1984) Geochemical modeling: a comparison of forward and inverse methods. In: Hitchon B, Wallick EI (eds) First Canadian/American conference on hydrogeology, practical applications of ground water geochemistry: Worthington. National Water Well Association, Oho, pp 149–177

Plummer, L.N., Prestemen, E.C. and Parkhurst, D. L. 1991. An interactive code (NETPATH) for modeling net geochemical reactions along a flow path. U. S. Geological Survey, Water Resources Investigations, Report 91–4078; P 93.

Qian, H., and Ma, Z. Y. 2005. Hydrogeochemistry. Beijing: Geological Publishing House.

Raju NJ, Shukla UK, Ram P (2011) Hydrogeochemistry for the assessment of groundwater quality in Varanasi: a fast-urbanizing center in Uttar Pradesh, India. Environ Monit Assess V 173:279–300

Sami, K. 2009. Groundwater exploration and development. The Basement Aquifers of Southern Africa Proceedings. Rian Titus, Hans Beekman, Shafick Adams and Leslie Strachan (editors), p. 19–30.

Senthilkumar M, Elango L (2013) Geochemical processes controlling the groundwater quality in lower Palar river basin, southern India. J. Earth Syst. Sci. 122. No 2:419–432

Seung-gu L, Tong-kwon K, Jin-soo L, Taejong L, Byongwook C, Heejae K (2008) Geochemical implication of 87Sr/86Sr ratio of high-temperature deep groundwater in a fractured granite aquifer. Geochem J 42:429–441

Singhal BBS, Gupta RP (1999) Applied hydrogeology of fractured rocks. Kluwer, Dordrecht, p 400

WHO, 2006. Guidelines for drinking water quality. World Health Organization, Geneva.

Zaidi FK, Ahmed S, Dewandel B, Maréchal JC (2007) Optimizing a piezometric network in the estimation of the groundwater budget: a case study from a crystalline-rock watershed in southern India. Hydrogeol J 15(6):1131–1145